Atmos. Chem. Phys. Discuss., 14, 26085–26125, 2014
www.atmos-chem-phys-discuss.net/14/26085/2014/
doi:10.5194/acpd-14-26085-2014

Atmospheric Chemistry and Physics Discussions

Simulating aerosol–radiation–cloud feedbacks on meteorology and air quality over eastern China under severe haze conditions in winter

B. Zhang[1,2], **Y. X. Wang**[1,3], **and J. M. Hao**[2]

[1]Ministry of Education Key Laboratory for Earth System Modeling, Center for Earth System Science, Institute for Global Change Studies, Tsinghua University, Beijing, 100084, China
[2]School of Environment, Tsinghua University, Beijing, 100084, China
[3]Department of Atmospheric Sciences, Texas A&M University, College Station, TX, 77843, USA

Received: 21 September 2014 – Accepted: 29 September 2014 – Published: 17 October 2014

Correspondence to: Y. X. Wang (yxw@mail.tsinghua.edu.cn)

Published by Copernicus Publications on behalf of the European Geosciences Union.

Abstract

The aerosol–radiation–cloud feedbacks on meteorology and air quality over eastern China under severe winter haze conditions during January 2013 are simulated using the fully coupled on-line Weather Research and Forecasting/Chemistry (WRF-Chem) model. Three simulation scenarios including different aerosol configurations are undertaken to distinguish the impact of aerosol radiative (direct and semi-direct) and indirect effects on meteorological variables and air quality. Simulated spatial and temporal variations of $PM_{2.5}$ are generally consistent with surface observations, with a mean bias of $-18.9\,\mu g\,m^{-3}$ ($-15.0\,\%$) averaged over 71 big cities in China. Comparisons between different scenarios reveal that aerosol radiative effects (direct effect and semi-direct effects) result in reductions of downward shortwave flux at the surface, 2 m temperature, 10 m wind speed and planetary boundary layer (PBL) height by up to $84.0\,W\,m^{-2}$, $3.2\,^{\circ}C$, $0.8\,m\,s^{-1}$, and 268 m, respectively. The simulated impact of the aerosol indirect effects is comparatively smaller. Through reducing the PBL height and wind speeds, the aerosol effects lead to increases in surface concentrations of primary pollutants (CO and SO_2) and $PM_{2.5}$. The aerosol feedbacks on secondary pollutants such as surface ozone and $PM_{2.5}$ mass concentrations show some spatial variations. Surface O_3 mixing ratio is reduced by up to 6.9 ppb due to reduced incoming solar radiation and lower temperature. Comparisons of model results with observations show that inclusion of aerosol feedbacks in the model significantly improves model's performances in simulating meteorological variables and improves simulations of $PM_{2.5}$ temporal distributions over the North China Plain, the Yangtze River Delta, the Pearl River Delta, and Central China. Although the aerosol–radiation–cloud feedbacks on aerosol mass concentrations are subject to uncertainties, this work demonstrates the significance of aerosol–radiation–cloud feedbacks for real-time air quality forecasting under haze conditions.

1 Introduction

Atmospheric aerosols are known to play a key role in the earth climate system. They absorb and scatter incoming solar radiation, referred to as direct effect (Hansen et al., 1997). They also alter cloud properties by serving as cloud condensation nuclei (CCN), which is known as indirect effect (Albrecht, 1989; Twomey, 1977; Rosenfeld et al., 2008). Absorbing aerosols in and under the cloud may also burn out the cloud (semi-direct effect) (Charlson and Pilat, 1969). It is of increasing interests to understand and quantify the complex impacts of aerosols on meteorology and air quality. The coupled "on-line" meteorology-air quality strategy with aerosol feedbacks is essential for real-time air quality forecasting using 3-D models. Negligence of aerosol feedbacks may lead to poor performance of the next hour's meteorology and air quality forecasting, especially for high aerosol loading regions (Grell and Baklanov, 2011; Zhang et al., 2012).

Models simulating aerosol direct, indirect, and semi-direct effects on meteorology and chemistry need to couple aerosols with physical and chemical processes. The chemistry version of Weather Research and Forecasting (WRF-Chem) model (Grell et al., 2005) is a state-of-the-art meso-scale "on-line" atmospheric model, in which the chemical processes and meteorology are simulated simultaneously. This design makes WRF-Chem capable of simulating aerosol feedbacks on various atmospheric processes. Several studies employing WRF-Chem reveal that aerosols reduce downward solar radiation reaching the ground, inhibit convections, reduce the PBL, and make the lower atmosphere more stable (Fan et al., 2008; Forkel et al., 2012; Zhang et al., 2010;). WRF-Chem results also indicate that aerosols can modify atmospheric circulation systems, resulting in changes in monsoon strength, precipitation distribution, and mid-latitude cyclones (Zhao et al., 2011, 2012).

In January 2013, several severe and long-lasting haze episodes appeared in eastern China (Fig. 1). Monthly mean mass concentrations of fine particulate matters ($PM_{2.5}$) exceeded 200 $\mu g\,m^{-3}$ in some cities in North China Plain. Meteorological conditions

and chemical components of $PM_{2.5}$ during this month have been investigated by a number of studies in order to understand the chemical characteristics and formation mechanism of severe winter haze episodes (Bi et al., 2014; Che et al., 2014; Huang et al., 2014; Sun et al., 2014; L. T. Wang et al., 2014; Y. S. Wang et al., 2014; Y. X. Wang et al., 2014; Z. F. Wang et al., 2014; J. K. Zhang et al., 2014). Meanwhile, such high levels of PM concentrations are expected to exert impacts on meteorological conditions through the aerosol–radiation–cloud interactions. Few current air quality forecasting systems for China include aerosol-meteorology interactions. The significance of this effect and the extent to which it feedbacks on air quality remains to be uncertain and needs to be quantified for better forecasting air quality in China in the future (Wang et al., 2013; Y. Zhang et al., 2014; Z. F. Wang et al., 2014).

In this work, the fully coupled "on-line" WRF-Chem model is employed to simulate the complex interactions between aerosols and meteorology and to characterize and quantify the influences of aerosol feedbacks on meteorology and air quality under severe winter haze conditions in January 2013 over eastern China. The aerosol direct, indirect and semi-direct effects are all included in the WRF-Chem simulation and analyzed separately. The WRF-Chem model configuration, scenarios setup, and observation data are described in Sect. 2. Section 3 evaluates the model in simulating meteorology and air quality. In Sect. 4, the aerosol feedbacks on meteorology and air quality are analyzed and discussed. Section 5 investigates the effects of including aerosol feedbacks in the model to the model's performances. The concluding remarks are given in Sect. 6.

2 Model and observations description

2.1 WRF-Chem model and scenarios setup

The WRF model is a state-of-the-art meso-scale non-hydrostatic model, and allows for many different choices for physical parameterizations (http://www.wrf-model.org/). WRF-Chem is a chemical version of WRF that simultaneously simulates meteorological

and chemical components. The version 3.3 of WRF-Chem released on 6 April 2011 is used in this study. A more detailed description of the model can be found in previous studies (Grell et al., 2005; Fast et al., 2006; Chapman et al., 2009).

The main physical options selected in this study include the Goddard shortwave radiation scheme coupled with aerosol direct effects (Chou et al., 1998), the Rapid Radiative Transfer Model (RRTM) longwave radiation scheme (Mlawer et al., 1997), the Noah Land Surface Model (Chen and Dudhia, 2001), the Yonsei University (YSU) boundary layer scheme (Hong et al., 2006), the Lin microphysics scheme coupled with aerosol indirect effects (Lin et al., 1983), and the Grell–Devenyi cumulus parameterization scheme (Grell and Dévényi, 2002).

The Carbon Bond Mechanism version Z (CBMZ) (Zaveri and Peters, 1999) is used as gas-phase chemistry scheme. The Model for Simulating Aerosol Interactions and Chemistry (MOSAIC) (Zaveri et al., 2008) is applied as aerosol module. MOSAIC simulates aerosol species such as sulfate, methanesulfonate, nitrate, ammonium, chloride, carbonate, sodium, calcium, black carbon (BC), organic carbon (OC), and other unspecified inorganic matters (OIN). Secondary organic aerosols are not included in the version of MOSAIC used in this study. MOSAIC in WRF-Chem uses a sectional approach to represent particle size distribution. In this study, four size bins (0.039–0.156, 0.156–0.625, 0.625–2.5, 2.5–10.0 µm dry diameter) are employed, and aerosols are assumed to be internally mixed within each bin.

The simulated time period is the whole month of January 2013. Figure 1 illustrates the model domain, which covers eastern China (19–51° N, 96–132° E) and has a horizontal resolution of 27 km × 27 km. There are 28 vertical levels extending from the surface to 50 hPa. The initial and boundary conditions for WRF are provided by the 6 hourly 1° × 1° National Centers for Environmental Prediction (NCEP) Final Analysis (FNL). Chemical boundary conditions are provided by MOZART simulations (Emmons et al., 2010). In the initial spin-up process, the model is run with NCEP meteorological and MOZART chemical conditions for 48 h. The model's meteorology is re-initialized every five days based on NCEP, while chemistry adopts the previous state.

In order to investigate the impact of aerosol feedbacks on meteorology and air quality, three WRF-Chem simulation scenarios are performed and compared. The first is the baseline scenario (BASE), including all aerosol effects on meteorology (i.e., direct, indirect, and semi-direct). The second scenario (RAD) focuses on the radiative effects by excluding aerosol indirect effects from the BASE scenario. The third scenario (EMP) does not contain any aerosol effects on meteorology. Other than the differences in aerosols effects, the three scenarios are identical in input data (e.g., emissions, boundary conditions, etc) and model setups. The difference between BASE and EMP (BASE – EMP) is used to investigate the impact of total aerosol feedbacks, while the difference between BASE and RAD (BASE – RAD) and that between RAD and EMP (RAD – EMP) represents the influence of aerosol indirect effects and radiative (both direct and semi-direct) effects, respectively. Table 1 summaries the characteristics of the three scenarios.

2.2 Emissions

Anthropogenic emissions are taken from the Multi-resolution Emission Inventory of China (MEIC) (http://www.meicmodel.org/), which provides emissions of sulfur dioxide (SO_2), nitrogen oxides (NO_x), carbon monoxide (CO), ammonia (NH_3), BC, OC, PM_{10}, $PM_{2.5}$, and non-methane volatile organic compounds (NMVOCs) for China for the year 2010. NO_x emissions contain 90 % of NO_2 and 10 % of NO by mole fraction. PM emissions are assumed to be split into 20 % in nuclei mode and 80 % in accumulation mode.

Biogenic emissions are calculated on-line in the model based on the Model of Emissions of Gases and Aerosols from Nature (MEGAN) inventory (Guenther et al., 2006). Dust is included in the simulations, while sea salt or dimethylsulfide (DMS) are not, and their impacts are expected to be small over eastern China in winter.

2.3 Observations

The simulation results are compared with meteorological and chemical observations. Daily meteorological observations at 523 stations are obtained from the National Climate Data Center (NCDC) of China Meteorological Administration (CMA), including 2 m temperature, 2 m relative humidity (RH), and 10 m wind speed. The radiosonde profiles at 20 stations are provided by the department of atmospheric science in University of Wyoming (http://weather.uwyo.edu/upperair/sounding.html).

The real-time hourly near surface $PM_{2.5}$ mass concentrations are obtained from China National Environmental Monitoring Center (CNEMC). The observation data were released since January 2013, including SO_2, NO_2, CO, Ozone (O_3), PM_{10} and $PM_{2.5}$ in 74 big cities in China. This database allows for a spatially extensive evaluation of air quality simulations by atmospheric models.

3 Model evaluations

Accurate representation of meteorology and aerosols distributions in the model provides the foundations of quantifying aerosol feedbacks. Therefore, in this section, the model performances are evaluated by comparing model results with surface and radiosonde observations. If not otherwise specified, the model results presented in this section are from BASE scenario, which represents the most comprehensive realization of different processes in the model. It should be noted that systematic differences may result from the comparison between grid-mean values and point measurements, since a model grid covers an area of 729 km^2 (27 km × 27 km).

3.1 Meteorology

Meteorology strongly affects formations, transportations, and eliminations of atmospheric aerosols. The selected near surface meteorological variables are 2 m temperature, 2 m relative humidity, and 10 m wind speed. Vertical profiles of temperature, rel-

ative humidity and wind speed are also compared. Figure 2 shows the time series of observed and simulated daily mean meteorological variables, with the statistical summary of the comparisons shown in Table 2. The model reproduces temporal variations of meteorological variables.

The statistical indices used here are mean observation (MEAN OBS), mean simulation (MEAN SIM), correlation coefficient (Corr. *R*), mean bias (MB), normalized mean bias (NMB), and root mean square error (RMSE). The definitions of these indices are given in the Appendix. The model reproduces 2 m temperature with a correlation of 0.97 and a cold bias of −1.0 °C, mainly due to underestimation in the first 9 days of the month. Relative humidity is simulated with a correlation of 0.47 and a negligible mean bias. The 10 m wind speed is systematically overestimated by the model by 105 %. This high positive bias in wind speed is also reported by several other studies using WRF-Chem (Matsui et al., 2009; Molders et al., 2012; Tuccella et al., 2012; Zhang et al., 2010).

Air pollution is influenced not only by surface meteorology, but also by vertical patterns of meteorological variables. In Fig. 3, the monthly mean vertical profiles of simulated meteorological variables are compared with sounding observations at 00:00 and 12:00 UTC. Generally, the model captures vertical variations of meteorological variables. The model well reproduces vertical variations of temperature with a small bias. The model underestimates relative humidity below 650 hPa and overestimates it in the upper levels. Wind speeds are overestimated in the lower atmosphere and underestimated in the upper atmosphere. The errors in meteorology may have influences on the accuracies of simulating processes of aerosol formation, transportation and deposition. Overall, the evaluations presented here suggest that the model adequately simulates the spatial and temporal variations of meteorological variables of significant relevance to air quality.

3.2 $PM_{2.5}$

We first evaluate the spatial distributions of simulated monthly mean $PM_{2.5}$ mass concentrations by comparing model results with observations at 71 big cities in the model domain in January 2013. As shown in Fig. 4, the model well captures the spatial patterns of $PM_{2.5}$ during the month, including high levels of $PM_{2.5}$ over southern Hebei, Henan, Hubei Province, Sichuan Basin and three big cities (Harbin, Changchun, Shenyang) in Northeast China. The North China Plain (NCP), Central China (CC) area, and Sichuan Basin have the highest monthly mean $PM_{2.5}$ mass concentrations. $PM_{2.5}$ pollution is more severe over the Yangtze River Delta (YRD) than that over the Pearl River Delta (PRD).

Figure 5 presents the scatter plots of observed and simulated monthly mean $PM_{2.5}$ mass concentrations at 71 cities. The model has a low bias ranging from 25 to 70 % for cities with monthly mean $PM_{2.5}$ exceeding 200 $\mu g\,m^{-3}$. The observed and simulated time-series of hourly surface $PM_{2.5}$ averaged over all the cities are compared in Fig. 6. The model simulates hourly $PM_{2.5}$ with a temporal correlation of 0.67, and underestimates monthly mean $PM_{2.5}$ mass concentrations by 18.9 $\mu g\,m^{-3}$ (15.0 %). The model generally reproduces the observed temporal variations of $PM_{2.5}$.

The enhancement ratio is employed to further evaluate the model's performances in simulating $PM_{2.5}$ temporal variations in different regions. The enhancement ratio is defined as the average of hourly $PM_{2.5}$ mass concentrations exceeding the median divided by that less than the median, representing changes of $PM_{2.5}$ from clean to polluted situations. As shown in Table 3, observed enhancement ratios are around 1.7 over NCP, YRD, PRD and CC. The simulated enhancement ratios range from 1.8 to 2.0 over the four regions, which are close to observations. Since changes of hourly emissions is not considered in this study, $PM_{2.5}$ enhancements mainly result from worsened meteorological conditions and more productions of secondary aerosols. The consistencies of simulated enhancement ratios with observed ones indicate the WRF-Chem model has

some success in simulating changes of aerosol related meteorological and chemical processes from clean to polluted situations.

However, the model fails to capture the extremely high values of $PM_{2.5}$ during the haze episodes in January 2013, for example, January 13–15 and January 18–20. Both positive and negative bias exists in simulated hourly $PM_{2.5}$. The model's underestimation during severe winter haze episodes is consistent with previous studies (Liu et al., 2010; L. T. Wang et al., 2014; Y. X. Wang et al., 2014; Zhou et al., 2014). Possible reasons for this underestimation are: (1) bias in simulating meteorological conditions during haze episodes, (2) uncertainties in emissions, (3) missing secondary organic aerosols in the MOSAIC mechanism; and (4) lack of formation mechanisms of secondary inorganic aerosols, like heterogeneous oxidation of SO_2 on the surface of particulate matters (Harris et al., 2013). By adjusting SO_2 and NO_x emissions according to surface observations and parameterizing the heterogeneous oxidation of SO_2 on deliquesced aerosols in GEOS-Chem model, Y. X. Wang et al. (2014) reported improvements of simulated $PM_{2.5}$ spatial distribution and an increase of 120 % in sulfate fraction in $PM_{2.5}$.

4 Aerosol feedbacks on meteorology and air quality

As seen in the previous section, the WRF-Chem model has shown some success in simulating meteorology and $PM_{2.5}$. Therefore, in this section, we aim to characterize and quantify the aerosol feedbacks on meteorology and air quality by comparing the three different scenarios described in Sect. 2.

In addition to different setups of the aerosol–radiation–cloud feedbacks, differences among the three scenarios can also result from model noise, such as errors in numerical computation and disturbances from discrete updating initial and boundary conditions. The Student's t test is employed to identify statistically significant differences between the scenarios. We only present and discuss aerosol-induced changes of meteorological and chemical variables which exceed 95 % confidence interval.

4.1 Feedbacks on meteorology

The evolution of atmospheric aerosols is strongly influenced by meteorological variables, such as solar radiation, air temperature, and wind speed, etc. Figure 7 illustrates aerosol impacts on downward shortwave flux at the ground, 2 m temperature, 10 m wind speed and PBL height over eastern China in January 2013. Downward shortwave flux at the ground is strongly influenced by the existence of atmospheric aerosols, especially over high aerosol-loading regions. Aerosols affect shortwave radiation reaching the ground in two ways. First, particles scatter and absorb incoming solar radiation directly, resulting in surface dimming. Second, in-cloud particles change cloud lifetime and albedo, thus causing variations of shortwave radiation at the ground surface. As in Fig. 7a, the downward shortwave flux at the ground is reduced over vast areas of eastern China by up to $-84.0\,W\,m^{-2}$, which mainly results from aerosol radiative effects (Fig. 7b). By employing ground-based measurements, aerosol optical and radiative properties over NCP during January 2013 were characterized in Bi et al. (2014) and Che et al. (2014). They reported strong negative aerosol direct radiative forcing at the surface (with maximum daily mean exceeding $-200.0\,W\,m^{-2}$), which our finding is consistent with. Forkel et al. (2012) simulated aerosol direct and indirect effects over Europe, where aerosol concentrations were relatively low ($PM_{2.5}$ = 10–20 $\mu g\,m^{-3}$), and suggested that the aerosol indirect effects dominated in aerosol feedbacks on downward shortwave flux at the ground. Different from Forkel et al. (2012), we find that aerosol indirect effects have little influence on the downward shortwave flux at the ground (not shown here). This may be explained that cloud is not so important in winter over the continent.

When the downward shortwave flux at the ground is decreased due to aerosol interception, near surface energy fluxes are suppressed, leading to a weaker convection. Near surface air is heated mainly by longwave radiation emitted from the ground. In that case, when shortwave flux at the ground is decreased, less longwave radiation is emitted from the surface and thus the near surface air is cooled. Due to a weaker

convection resulted from less shortwave radiation reaching the ground, 2 m temperature is reduced by up to 3.2 °C, 10 m wind speed is reduced by up to $0.8\,m\,s^{-1}$, and PBL height is also reduced by up to 268 m, as shown in Fig. 7c, e and g, respectively. Meteorological variables such as air temperature, wind speed, and PBL height could also be influenced by other factors like land surface properties (Zhang et al., 2010), other than solar radiations. So that changes of these variables, especially wind speed, are less significant than solar radiation. However, the spatial patterns of changes of these variables are consistent with that of downward shortwave flux, which indicates that a more stable lower atmosphere resulting from less shortwave radiation plays an important role in aerosol feedbacks. The aerosol indirect effects during severe haze episode are found to be not significant in altering solar radiation, temperature, wind speed or PBL height over eastern China, which is not shown here. Overall, the near surface atmosphere is more stable when aerosol feedback is considered in the model, which is conductive for pollution accumulation.

The amount of precipitation is low in January for most regions in China (Wang and Zhou, 2005). Cloud and precipitation formations mainly occur over areas in the south and over the ocean (Fig. 8a and d). In this month, the changes of cloud and precipitation due to aerosol radiative effects are not significant (Fig. 8h). Aerosol indirect effects directly alter cloud properties such as effective radius, cloud lifetime, and precipitation rate. As shown in Fig. 8i, aerosol indirect effects play a much more significant role in changing cloud properties. Cloud water path is greatly reduced by up to $5.7\,kg\,m^{-2}$ over the junction of Yunnan and Guizhou Province and ocean around Taiwan. The reduction over these relatively clean areas may be explained by the lower particle number concentrations in the BASE scenario than the default droplet number mixing ratio of $1.0 \times 10^6\,kg^{-1}$ in scenarios without aerosol indirect effect. Reduced cloud droplet number results in accelerating auto-conversion to rain droplets. Thus, simulated monthly precipitation is increased by almost 100 % over these areas (Fig. 8j). Similar results are found when we replace the Lin microphysics scheme by the two-moment Morrison scheme (Morrison et al., 2009). Previous model assessments also showed that

the inclusion of aerosol indirect effect reduced cloud water content over South Pacific ocean and made model simulations match better with aircraft observations (Yang et al., 2011). The relatively small precipitation, as well as small changes of precipitation due to aerosol feedbacks over the most parts of the domain, suggests that precipitation has a minor effect on near surface aerosols in January 2013.

4.2 Feedbacks on air quality

Through moderating meteorological variables, aerosols exert feedbacks on air quality. Figure 9 shows spatial distributions of CO, SO_2, and O_3 and aerosol feedbacks on the three gas pollutants in January 2013. Spatial patterns of CO and SO_2 are similar with that of $PM_{2.5}$, indicating similar sources of these pollutants. The near surface CO and SO_2 concentrations are increased when aerosol feedbacks are included. CO is enhanced by up to 446 ppb, while SO_2 is increased by as much as 28 ppb. Large increases of CO and SO_2 are found over areas with high aerosol loading. This phenomenon may mainly result from lower PBL and a more stable atmosphere near the surface due to aerosol radiative effects, as discussed in Sect. 3.2. We also found aerosol indirect effects do not have significant influence on gas pollutants.

The formation of O_3 is directly related to solar radiation and temperature in regions with sufficient NO_x and VOCs. The lower air temperature and reduced incoming solar radiation as a result of aerosols radiative effects lead to reduced photolysis rate of NO_2 and consequently reduce O_3 concentrations. The largest suppression of surface ozone by aerosols is found to be up to −6.9 ppb in the warmer southern China. Changes in northern China are relatively small. These findings are similar to those in Zhang et al. (2010) and Forkel et al. (2012).

The aerosol–radiation–cloud feedbacks on near surface aerosol mass concentrations are illustrated in Fig. 10. As shown in Fig. 10a, both increases and decreases of $PM_{2.5}$ are found in the domain. Enhanced $PM_{2.5}$ mass concentrations are simulated over Henan, Hubei, Guangxi Province, and Sichuan Basin with the maximum enhancement of 69.3 $\mu g\,m^{-3}$. Reduction in $PM_{2.5}$ as much as $-38.2\,\mu g\,m^{-3}$ are simulated over

Bohai Sea surrounding area, Northeast China and the conjunction area of Yunnan, Guangxi, and Guizhou Province (Southwest China).

In order to better understand mechanisms of how $PM_{2.5}$ respond to aerosol feedbacks, aerosol effects are divided into aerosol radiative effects (Fig. 10b) and indirect effects (Fig. 10c). $PM_{2.5}$ can be influenced by changes in various atmospheric processes due to aerosol radiative effects. For example, lower temperature may suppress the formation of sulfate, and reduced solar radiation may inhibit the oxidations of precursors of secondary aerosols. Among the various changes in atmospheric processes, the reduced PBL height and the stabilized lower atmosphere is the most important. From Fig. 11b, we can see that $PM_{2.5}$ is greatly increased by aerosol radiative effects over the region where solar radiation and PBL height are significantly reduced during winter haze (Fig. 7a and g). The mechanism involved is that aerosol radiative effects stabilize the lower atmosphere and suppress the dilution and ventilation of PM, which is the same situation for primary gas pollutants.

The comparison between Fig. 10a and c indicates that aerosol indirect effects are the main reason of the suppression of $PM_{2.5}$. The reduction of $PM_{2.5}$ in WRF-Chem simulations with aerosol indirect effects mainly comes from two aspects. First, once aerosol indirect effects are included in the model, the cloud droplet number is based on simulated atmospheric aerosol number other than prescribed in scenarios without indirect effects. This coding strategy allows interstitial air-borne aerosols to become cloud-borne aerosols after activation. Therefore, air-borne aerosols are reduced in simulations including aerosol indirect effects, especially over cloudy regions like southwestern China (Fig. 8a). Second, in the simulations including aerosol indirect effects, a more comprehensive in- and below-cloud aerosol wet removal module following the method of Easter et al. (2004) is employed, while in the simulations without aerosol indirect effects, this module is not activated. In this aerosol wet removal mechanism, the removal processes are assumed to be irreversible, and aerosol re-suspension is not considered, even when precipitation is weak. This leads to a stronger removal of atmospheric aerosols when including aerosol indirect effects. It should be noted that

in this work, the enhancement of aerosol wet removal process, when including aerosol indirect effects in the model, mainly results from WRF-Chem model configurations, not from aerosol-induced changes in cloud properties or precipitation.

The above discussion is based on model results temporally averaged during the whole month. In order to better understand $PM_{2.5}$ variations on a day to day basis, 4 cities with significant $PM_{2.5}$ enhancements and 4 cities with significant $PM_{2.5}$ reductions are selected. Figure 11 shows the time series of observed and simulated hourly surface $PM_{2.5}$ mass concentrations in the selected 8 cities in January 2013. The four cites with increasing monthly mean $PM_{2.5}$ due to aerosol feedbacks are Zhengzhou, Wuhan, Changsha, and Chengdu. Major enhancements of $PM_{2.5}$ are simulated when $PM_{2.5}$ levels are high, for example, during the period of 15–17 January The changes in $PM_{2.5}$ has a moderate negative correlation with the changes in PBL height (correlations coefficient ≈ -0.3) at the four cites, suggesting that the $PM_{2.5}$ enhancement is partly caused by decreased PBL height in these regions. Suppressions of $PM_{2.5}$ in Qinhuangdao, Tianjin, Shenyang, and Changchun, which are the four cities with decreased monthly mean $PM_{2.5}$, mainly happen in the last 5 days of the month (26–31 January).

In summary, aerosol radiative effects reduce the downward shortwave flux at the ground, decrease near surface temperature and wind speed, and further weaken convection, all leading to a more stable lower atmosphere. In a more stable lower atmosphere due to aerosol radiative effects, primary gas pollutants (CO and SO_2) and $PM_{2.5}$ are enhanced, while O_3 is decreased because of less incoming solar radiation and lower temperatures. $PM_{2.5}$ are suppressed when aerosol indirect effects are included, mainly due to the transition from air-borne aerosol to cloud-borne aerosol and the activation of a more comprehensive aerosol wet removal module. The underestimations at the higher end indicate that some key mechanisms are missing in the model, especially the productions of secondary aerosols.

5 Effects of including aerosol feedbacks on model's performances

In previous sections, the model results are evaluated, and the aerosol feedbacks on meteorology and air quality are characterized and quantified. Atmospheric aerosols during severe winter haze episodes bring along changes of incoming solar radiation, near surface temperature, PBL height and lower atmosphere stability, which is discussed in Sect. 4. Furthermore, these changes of meteorological variables increase or decrease near surface $PM_{2.5}$ concentrations through direct or indirect influences. For example, reductions of PBL height and stabilized lower atmosphere increase near surface $PM_{2.5}$ concentrations, while lower temperature inhibits productions of secondary aerosols. Therefore, whether or not inclusions of aerosol feedbacks in the model improves model's performances in simulating severe winter haze episodes is not obvious and need to be investigated.

In this section we address the question whether including aerosol feedbacks within the model improves model's performances in simulating severe haze episodes. Model results from the BASE (with all aerosol feedbacks) and EMP (without any aerosol feedbacks) scenarios are compared with observations to evaluate which scenario is more consistent with reality.

As an example to shown the extent to which simulated meteorological variables are affected by including aerosol feedbacks, Fig. 12 compares downward shortwave radiation at the ground and temperature between the BASE and EMP scenario over NCP, where $PM_{2.5}$ pollution is most severe in January 2013. Both scenarios have a high bias in daily total shortwave radiation at the ground, mainly due to the overestimation of maximum shortwave radiation at noon (Z. F. Wang et al., 2014). However, the inclusion of aerosol feedbacks leads to a 22 % reduction of the normalized mean bias. The model prediction of 2 m temperature is also improved in the scenario with aerosol feedbacks during haze episodes, such like 12–15 and 19–24 January. These findings are consistent with the results in Z. F. Wang et al. (2014), indicating the importance

of including aerosol feedbacks in simulating meteorology under high aerosol loading conditions.

Figures 5 and 6 compare simulated $PM_{2.5}$ over 71 big cities in January 2013 in BASE and EMP scenarios averaged temporally and spatially, respectively. However, no significant improvements are found when aerosol feedbacks are included, partially due to the missing of smaller scale temporal and spatial information averaging. So we further investigate the model's performances in simulating $PM_{2.5}$ over several important regions. Box plots of monthly mean $PM_{2.5}$ mass concentrations in January 2013 over NCP, YRD, PRD and CC are displayed in Fig. 12. Over all the four areas, the median values of hourly $PM_{2.5}$ are underestimated in scenario EMP, in which aerosol feedbacks are excluded. Biases of the median values in EMP scenario are −29.1, −16.8, −10.7, −5.3 % over NCP, YRD, PRD, and CC, respectively. Simulations of hourly $PM_{2.5}$ mass concentration distributions are improved when aerosol feedbacks are included in BASE scenario in two aspects. First, biases of the median values are reduced to −22.0, −12.0, −6.7, +2.6 % over NCP, YRD, PRD, and CC, respectively. Second, the distribution of middle 50 % (ranging from 25th percentile to 75th percentile) hourly $PM_{2.5}$ mass concentrations is more consistent with observations than without aerosol feedbacks in the model. We also find an positive feedback for $PM_{2.5}$. That is, aerosols increase $PM_{2.5}$ through meteorological and chemical processes.

Overall in this section, we demonstrate the significance of including aerosol feedbacks in the model. Inclusions of aerosol feedbacks in the model reproduce aerosol effects on solar radiation and temperature. Thus, biases of simulated meteorology are reduced. Though reactions of $PM_{2.5}$ to aerosol feedbacks are complex, inclusions of aerosol feedbacks improves model's performances to some extent in simulating $PM_{2.5}$ in winter haze conditions.

6 Conclusions

In this work, the fully coupled on-line WRF-Chem model is applied to investigate aerosol–radiation–cloud feedbacks on meteorology and air quality over eastern China in January 2013, in which month China experienced the most severe haze pollution in history. Three simulation scenarios including different aerosol configurations are undertaken and compared.

Results in the baseline simulation show that the model well captures temporal and vertical variations of meteorological variables, except for overestimating lower atmosphere wind speed which is a common issue for the WRF-Chem model. The model reproduces spatial distribution of monthly mean $PM_{2.5}$ mass concentration, with high aerosol concentrations over southern Hebei, Henan, Hubei Province, Sichuan Basin and three big cities (Harbin, Changchun, Shenyang) in Northeast China. Monthly mean $PM_{2.5}$ averaged over 71 big cities is underestimated by 15 %. The model tends to underestimate $PM_{2.5}$ at the high ends, which is a common problem models are facing with in simulating haze conditions. Further studies improving model abilities in simulating high aerosol pollution are needed.

Previous work indicated that the influences on air quality meteorology of aerosol indirect effects are larger than radiative effects, but this was derived under conditions with much lower aerosol loadings than those in our study. In this work we find that under winter haze conditions, aerosol radiative effects (direct effect and semi-direct effects) play a dominant role in modulating downward shortwave flux at the ground surface, lower atmosphere temperature, wind speed and PBL height. These four meteorological variables are reduced by up to 84.0 $W\,m^{-2}$, 3.2 °C, 0.8 $m\,s^{-1}$, and 268 m, respectively. However, aerosol indirect effects are more important than radiative effects in altering cloud properties and precipitation.

The lower PBL and smaller wind speed result in increases of near surface CO and SO_2 concentrations. Higher aerosol loading reduces solar radiation and temperature at the surface, which results in a reduction of NO_2 photolysis rate and subsequently

a reduction in a reduction of O_3 mixing ratios by up to 6.9 ppb. The aerosol feedbacks on $PM_{2.5}$ concentrations exhibit large spatial variations. Both increases and decreases of $PM_{2.5}$ are found in the domain. The enhancements of $PM_{2.5}$ over Henan, Hubei Province, and Sichuan Basin by up to 17.8 $\mu g\,m^{-3}$ are mainly due to large reduction of PBL height in these areas. The suppressions of $PM_{2.5}$ over Bohai Sea surrounding area, Northeast China, and Southwestern China are resulted from the transition from air-borne aerosol to cloud-borne aerosol and the activation of a more comprehensive aerosol wet removal module.

The inclusion of aerosol feedback improves the model's ability in simulating downward shortwave radiation and temperature. Simulations of hourly $PM_{2.5}$ mass concentration distributions over NCP, YRD, PRD, and CC, are also improved when aerosol feedbacks are included. These indicates the importance of involving aerosol–radiation–cloud interactions in modeling air quality meteorology.

There are a number of limitations in this work. The relative coarse grid (27 km), the uncertainty of emission inventory, and the lack of secondary organic matters all contribute to the uncertainties in simulating aerosols. Also, one month length simulation could not represent a full view of aerosol–radiation–cloud feedbacks. Better understandings in the future are expected by applying more comprehensive aerosol treatments and a longer time period. Previous studies mainly focus on mechanisms of severe winter haze formation. Different from them, this work demonstrates the importance of aerosol feedbacks on meteorology and air quality during severe winter haze periods.

Appendix A:

The statistical indices used in this study are defined as following.
Mean Bias (MB)

$$\mathrm{MB} = 1/N \sum_{i=1}^{N} (M_i - O_i)$$

Normalized Mean Bias (NMB)

$$\mathrm{NMB} = \frac{\sum_{i=1}^{N} (M_i - O_i)}{\sum_{i=1}^{N} O_i} \times 100\,\%$$

Correlation Coefficient (Corr. R)

$$\mathrm{Corr.}\ R = \frac{\sum_{i=1}^{N} \left(M_i - \overline{M}\right)\left(O_i - \overline{O}\right)}{\sqrt{\sum_{i=1}^{N} \left(M_i - \overline{M}\right)^2} \sqrt{\sum_{i=1}^{N} \left(O_i - \overline{O}\right)^2}}$$

Root Mean Square Error (RMSE)

$$\mathrm{RMSE} = \sqrt{1/N \sum_{i=1}^{N} (M_i - O_i)^2}$$

where $\overline{M} = 1/N \sum_{i=1}^{N} M_i$, $\overline{O} = 1/N \sum_{i=1}^{N} O_i$, $\overline{M}$ and $\overline{O}$ are model result and observation for sample i, respectively. N is the number of samples.

Acknowledgements. This research was supported by the National Key Basic Research Program of China (2014CB441302), the CAS Strategic Priority Research Program (Grant No. XDA05100403), and the Beijing Nova Program (Z121109002512052).

References

Albrecht, B. A.: Aerosols, cloud microphysics, and fractional cloudiness, Science, 245, 1227–1230, 1989.

Bi, J., Huang, J., Hu, Z., Holben, B. N., and Guo, Z.: Investigate the aerosol optical and radiative characteristics of heavy haze episodes in Beijing during January of 2013, J. Geophys. Res.-Atmos., 9884–9900, doi:10.1002/2014JD021757, 2014.

Chapman, E. G., Gustafson Jr., W. I., Easter, R. C., Barnard, J. C., Ghan, S. J., Pekour, M. S., and Fast, J. D.: Coupling aerosol–cloud–radiative processes in the WRF-Chem model: Investigating the radiative impact of elevated point sources, Atmos. Chem. Phys., 9, 945–964, doi:10.5194/acp-9-945-2009, 2009.

Charlson, R. and Pilat, M.: Climate: the influence of aerosols, J. Appl. Meteorol., 8, 1001–1002, 1969.

Che, H., Xia, X., Zhu, J., Li, Z., Dubovik, O., Holben, B., Goloub, P., Chen, H., Estelles, V., Cuevas-Agulló, E., Blarel, L., Wang, H., Zhao, H., Zhang, X., Wang, Y., Sun, J., Tao, R., Zhang, X., and Shi, G.: Column aerosol optical properties and aerosol radiative forcing during a serious haze-fog month over North China Plain in 2013 based on ground-based sunphotometer measurements, Atmos. Chem. Phys., 14, 2125–2138, doi:10.5194/acp-14-2125-2014, 2014.

Chen, F. and Dudhia, J.: Coupling an advanced land surface–hydrology model with the Penn State-NCAR MM5 modeling system. Part I: Model implementation and sensitivity, Mon. Weather Rev., 129, 569–585, 2001.

Chou, M.-D., Suarez, M. J., Ho, C.-H., and Yan, M. M.-H.: Parameterizations for cloud overlapping and shortwave single-scattering properties for use in general circulation and cloud ensemble models, J. Climate, 11, 202–214, doi:10.1175/1520-0442(1998)011<0202:PFCOAS>2.0.CO;2, 1998.

Emmons, L. K., Walters, S., Hess, P. G., Lamarque, J.-F., Pfister, G. G., Fillmore, D., Granier, C., Guenther, A., Kinnison, D., Laepple, T., Orlando, J., Tie, X., Tyndall, G., Wiedinmyer, C., Baughcum, S. L., and Kloster, S.: Description and evaluation of the Model for Ozone and Related chemical Tracers, version 4 (MOZART-4), Geosci. Model Dev., 3, 43–67, doi:10.5194/gmd-3-43-2010, 2010.

Fan, J., Zhang, R., Tao, W. K., and Mohr, K. I.: Effects of aerosol optical properties on deep convective clouds and radiative forcing, J. Geophys. Res.-Atmos., 113, D08209, doi:10.1029/2007JD009257, 2008.

Fast, J. D., Gustafson, W. I., Easter, R. C., Zaveri, R. A., Barnard, J. C., Chapman, E. G., Grell, G. A., and Peckham, S. E.: Evolution of ozone, particulates, and aerosol direct radiative forcing in the vicinity of Houston using a fully coupled meteorology–chemistry–aerosol model, J. Geophys. Res.-Atmos., 111, D21305, doi:10.1029/2005JD006721, 2006.

Forkel, R., Werhahn, J., Hansen, A. B., McKeen, S., Peckham, S., Grell, G., and Suppan, P.: Effect of aerosol–radiation feedback on regional air quality – a case study with WRF/Chem, Atmos. Environ., 53, 202–211, 2012.

Grell, G. and Baklanov, A.: Integrated modeling for forecasting weather and air quality: a call for fully coupled approaches, Atmos. Environ., 45, 6845–6851, doi:10.1016/j.atmosenv.2011.01.017, 2011.

Grell, G. A. and Dévényi, D.: A generalized approach to parameterizing convection combining ensemble and data assimilation techniques, Geophys. Res. Lett., 29, 38-31–38-34, 2002.

Grell, G. A., Peckham, S. E., Schmitz, R., McKeen, S. A., Frost, G., Skamarock, W. C., and Eder, B.: Fully coupled "online" chemistry within the WRF model, Atmos. Environ., 39, 6957–6975, 2005.

Guenther, A., Karl, T., Harley, P., Wiedinmyer, C., Palmer, P. I., and Geron, C.: Estimates of global terrestrial isoprene emissions using MEGAN (Model of Emissions of Gases and Aerosols from Nature), Atmos. Chem. Phys., 6, 3181–3210, doi:10.5194/acp-6-3181-2006, 2006.

Hansen, J., Sato, M., and Ruedy, R.: Radiative forcing and climate response, J. Geophys. Res.-Atmos., 102, 6831–6864, 1997.

Harris, E., Sinha, B., van Pinxteren, D., Tilgner, A., Fomba, K. W., Schneider, J., Roth, A., Gnauk, T., Fahlbusch, B., and Mertes, S.: Enhanced role of transition metal ion catalysis during in-cloud oxidation of SO_2, Science, 340, 727–730, 2013.

Hong, S.-Y., Noh, Y., and Dudhia, J.: A new vertical diffusion package with an explicit treatment of entrainment processes, Mon. Weather Rev., 134, 2318–2341, doi:10.1175/MWR3199.1, 2006.

Huang, K., Zhuang, G., Wang, Q., Fu, J. S., Lin, Y., Liu, T., Han, L., and Deng, C.: Extreme haze pollution in Beijing during January 2013: chemical characteristics, formation mechanism and role of fog processing, Atmos. Chem. Phys. Discuss., 14, 7517–7556, doi:10.5194/acpd-14-7517-2014, 2014.

Lin, Y.-L., Farley, R. D., and Orville, H. D.: Bulk parameterization of the snow field in a cloud model, J. Clim. Appl. Meteorol., 22, 1065–1092, 1983.

Liu, X.-H., Zhang, Y., Cheng, S.-H., Xing, J., Zhang, Q., Streets, D. G., Jang, C., Wang, W.-X., and Hao, J.-M.: Understanding of regional air pollution over China using CMAQ, Part I Performance evaluation and seasonal variation, Atmos. Environ., 44, 2415–2426, 2010.

Matsui, H., Koike, M., Kondo, Y., Takegawa, N., Kita, K., Miyazaki, Y., Hu, M., Chang, S. Y., Blake, D. R., Fast, J. D., Zaveri, R. A., Streets, D. G., Zhang, Q., and Zhu, T.: Spatial and temporal variations of aerosols around Beijing in summer 2006: model evaluation and source apportionment, J. Geophys. Res.-Atmos., 114, D00G13, doi:10.1029/2008jd010906, 2009.

Mlawer, E. J., Taubman, S. J., Brown, P. D., Iacono, M. J., and Clough, S. A.: Radiative transfer for inhomogeneous atmospheres: RRTM, a validated correlated-*k* model for the longwave, J. Geophys. Res.-Atmos., 102, 16663–16682, 1997.

Molders, N., Tran, H. N. Q., Cahill, C. F., Leelasakultum, K., and Tran, T. T.: Assessment of WRF/Chem $PM_{2.5}$ forecasts using mobile and fixed location data from the Fairbanks, Alaska winter 2008/09 field campaign, Atmos. Pollut. Res., 3, 180–191, doi:10.5094/apr.2012.018, 2012.

Morrison, H., Thompson, G., and Tatarskii, V.: Impact of cloud microphysics on the development of trailing stratiform precipitation in a simulated squall line: comparison of one-and two-moment schemes, Mon. Weather Rev., 137, 991 C1007, doi:10.1175/2008MWR2556.1, 2009.

Rosenfeld, D., Lohmann, U., Raga, G. B., O'Dowd, C. D., Kulmala, M., Fuzzi, S., Reissell, A., and Andreae, M. O.: Flood or drought: how do aerosols affect precipitation?, Science, 321, 1309–1313, 2008.

Sun, Y., Jiang, Q., Wang, Z., Fu, P., Li, J., Yang, T., and Yin, Y.: Investigation of the sources and evolution processes of severe haze pollution in Beijing in January 2013, J. Geophys. Res.-Atmos., 119, 4380–4398, doi:10.1002/2014JD021641, 2014.

Tuccella, P., Curci, G., Visconti, G., Bessagnet, B., Menut, L., and Park, R. J.: Modeling of gas and aerosol with WRF/Chem over Europe: evaluation and sensitivity study, J. Geophys. Res.-Atmos., 117, D03303, doi:10.1029/2011jd016302, 2012.

Twomey, S.: The influence of pollution on the shortwave albedo of clouds, J. Atmos. Sci., 34, 1149–1152, 1977.

Wang, H., Zhang, X., Gong, S., and Xue, M.: The simulation study of the interaction between aerosols and heavy air pollution weather in East China, AIP Conf. Proc., 1527, 499–502, doi:10.1063/1.4803314, 2013.

Wang, L. T., Wei, Z., Yang, J., Zhang, Y., Zhang, F. F., Su, J., Meng, C. C., and Zhang, Q.: The 2013 severe haze over southern Hebei, China: model evaluation, source apportionment, and policy implications, Atmos. Chem. Phys., 14, 3151–3173, doi:10.5194/acp-14-3151-2014, 2014.

Wang, Y. and Zhou, L.: Observed trends in extreme precipitation events in China during 1961–2001 and the associated changes in large-scale circulation, Geophys. Res. Lett., 32, L09707, doi:10.1029/2005GL022574, 2005.

Wang, Y. S., Yao, L., Wang, L., Liu, Z., Ji, D., Tang, G., Zhang, J., Sun, Y., Hu, B., and Xin, J.: Mechanism for the formation of the January 2013 heavy haze pollution episode over central and eastern China, Sci. China Ser. D, 1–12, 2014.

Wang, Y. X., Zhang, Q., Jiang, J., Zhou, W., Wang, B., He, K., Duan, F., Zhang, Q., Philip, S., and Xie, Y.: Enhanced sulfate formation during China's severe winter haze episode in Jan 2013 missing from current models, J. Geophys. Res.-Atmos., 119, 10425–10440, doi:10.1002/2013JD021426, 2014.

Wang, Z. F., Li, J., Wang, Z., Yang, W., Tang, X., Ge, B., Yan, P., Zhu, L., Chen, X., and Chen, H.: Modeling study of regional severe hazes over mid-eastern China in January 2013 and its implications on pollution prevention and control, Sci. China Ser. D, 57, 3–13, 2014.

Yang, Q., Gustafson Jr., W. I., Fast, J. D., Wang, H., Easter, R. C., Morrison, H., Lee, Y.-N., Chapman, E. G., Spak, S. N., and Mena-Carrasco, M. A.: Assessing regional scale predictions of aerosols, marine stratocumulus, and their interactions during VOCALS-REx using WRF-Chem, Atmos. Chem. Phys., 11, 11951–11975, doi:10.5194/acp-11-11951-2011, 2011.

Zaveri, R. A. and Peters, L. K.: A new lumped structure photochemical mechanism for large-scale applications, J. Geophys. Res.-Atmos., 104, 30387–30415, 1999.

Zaveri, R. A., Easter, R. C., Fast, J. D., and Peters, L. K.: Model for simulating aerosol interactions and chemistry (MOSAIC), J. Geophys. Res.-Atmos., 113, D13204, doi:10.1029/2007JD008782, 2008.

Zhang, J. K., Sun, Y., Liu, Z. R., Ji, D. S., Hu, B., Liu, Q., and Wang, Y. S.: Characterization of submicron aerosols during a month of serious pollution in Beijing, 2013, Atmos. Chem. Phys., 14, 2887–2903, doi:10.5194/acp-14-2887-2014, 2014.

Zhang, Y., Wen, X.-Y., and Jang, C.: Simulating chemistry–aerosol–cloud–radiation–climate feedbacks over the continental US using the online-coupled Weather Research Forecasting Model with chemistry (WRF/Chem), Atmos. Environ., 44, 3568–3582, 2010.

Zhang, Y., Bocquet, M., Mallet, V., Seigneur, C., and Baklanov, A.: Real-time air quality forecasting, part I: History, techniques, and current status, Atmos. Environ., 60, 632–655, doi:10.1016/j.atmosenv.2012.06.031, 2012.

Zhang, Y., Zhang, X., Cai, C., Wang, K., and Wang, L.: Studying aerosol–cloud–climate interactions over East Asia using WRF/Chem, in: Air Pollution Modeling and its Application XXIII, Springer, 61–66, 2014.

Zhao, C., Liu, X., Ruby Leung, L., and Hagos, S.: Radiative impact of mineral dust on monsoon precipitation variability over West Africa, Atmos. Chem. Phys., 11, 1879–1893, doi:10.5194/acp-11-1879-2011, 2011.

Zhao, C., Liu, X., and Leung, L. R.: Impact of the Desert dust on the summer monsoon system over Southwestern North America, Atmos. Chem. Phys., 12, 3717–3731, doi:10.5194/acp-12-3717-2012, 2012.

Zhou, G., Yang, F., Geng, F., Xu, J., Yang, X., and Tie, X.: Measuring and modeling aerosol: relationship with Haze Events in Shanghai, China, Aerosol Air Qual. Res., 14, 783–792, 2014.

Table 1. Summary of three simulated scenarios.

CASE name	Characteristics
BASE	With all aerosol feedbacks
RAD	Only with aerosol direct and semi-direct effects
EMP	Without any aerosol feedbacks

Table 2. Statistical Performance of baseline simulations for meteorology.

	T2 (°C)	RH2 (%)	WS10 ($m\,s^{-1}$)	$PM_{2.5}$ ($\mu g\,m^{-3}$)
N of stations	523	523	523	71
Mean OBS	−1.8	66	1.9	129.2
Mean SIM	−2.8	66	3.9	111.5
Corr. *R*	0.96	0.47	0.47	0.67
MB	−1.0	0	2.0	−18.9
NMB	−83.3 %	< 0.1 %	105 %	−15.0 %
RMSE	3.4	16	2.7	30.7

Table 3. Observed and simulated enhancement ratios of $PM_{2.5}$. The enhancement ratio is defined as the average of hourly $PM_{2.5}$ larger than the median value divided by that of hourly $PM_{2.5}$ less than the median value during the month. NCP, YRD, PRD, and CC represent the North China Plain, the Yangtze River Delta, the Pearl River Delta, and Central China, respectively.

	NCP	YRD	PRD	CC
Observations	1.8	1.7	1.7	1.7
WRF-Chem (BASE)	1.8	2.0	1.8	2.0

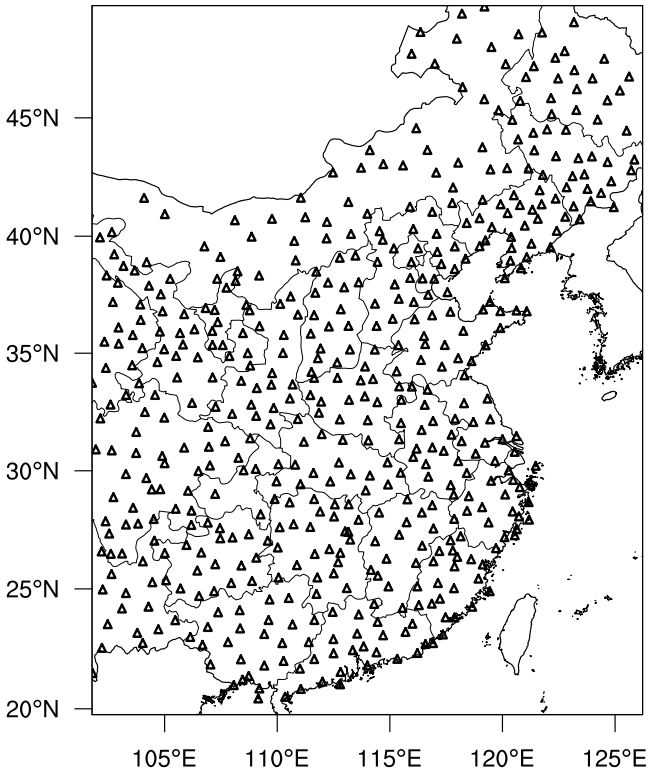

Figure 1. WRF/Chem modeling domain with grid resolution of 27 km. The domain covers eastern parts of China. The triangles indicates the location of 523 meteorology stations used for evaluations in this work.

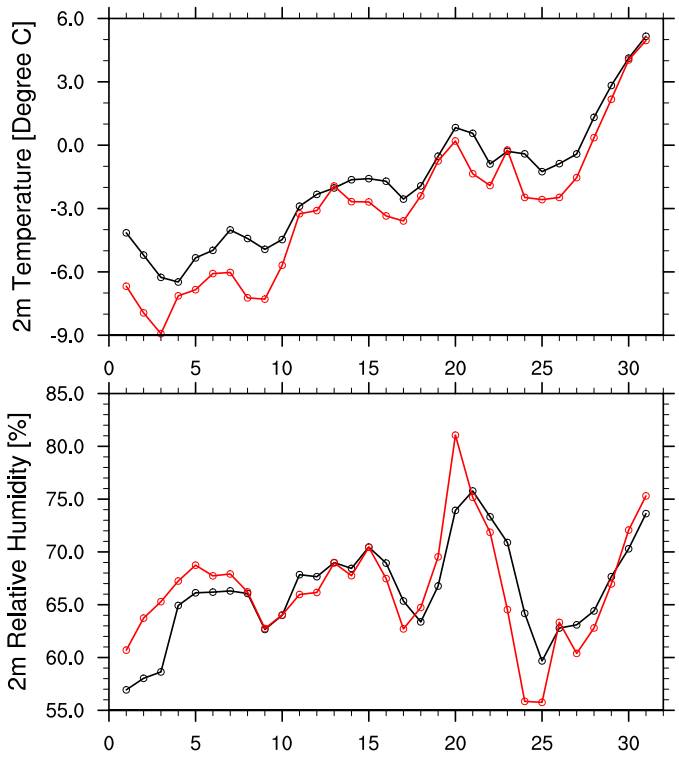

Figure 2. Time series of observed (black line) and simulated (red line) daily meteorological variables averaged over 523 meteorology stations in January 2013.

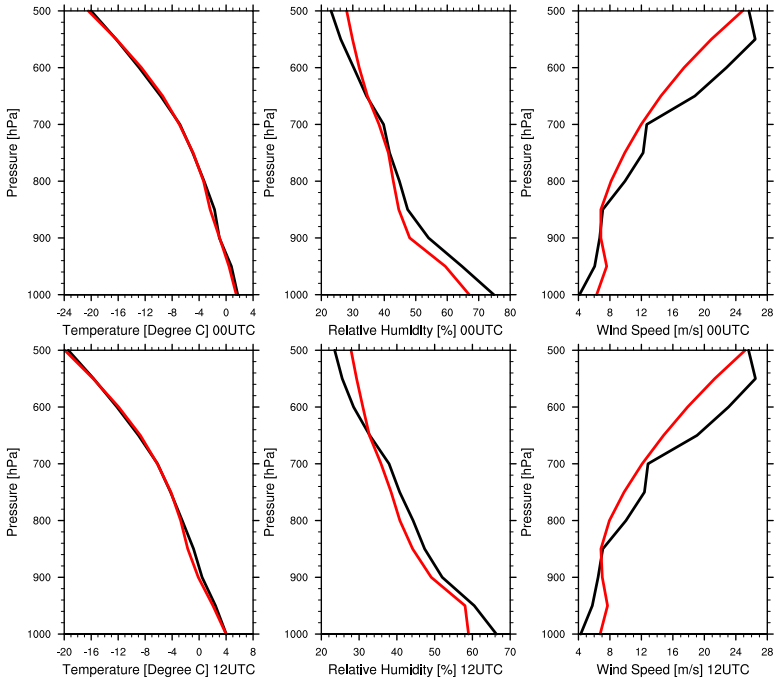

Figure 3. Monthly mean vertical profiles of observed (black line) and simulated (red line) meteorological variables averaged over 36 meteorology stations.

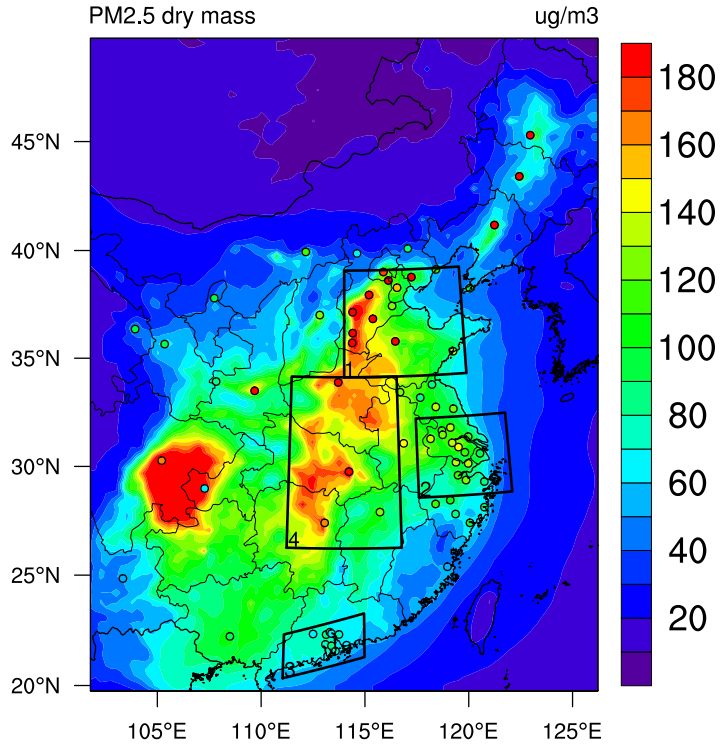

Figure 4. Simulated and Observed (circles) monthly mean $PM_{2.5}$ mass concentration over eastern China in January 2013. The four polygons stands for the North China Plain (NCP) (#1), the Yangtze River Delta (YRD) (#2), the Pearl River Delta (PRD) (#3), and Central China (#4).

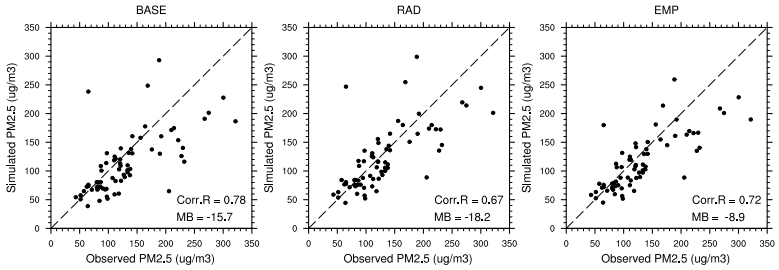

Figure 5. Scatter plots of monthly mean $PM_{2.5}$ mass concentrations in 71 cities in January 2013.

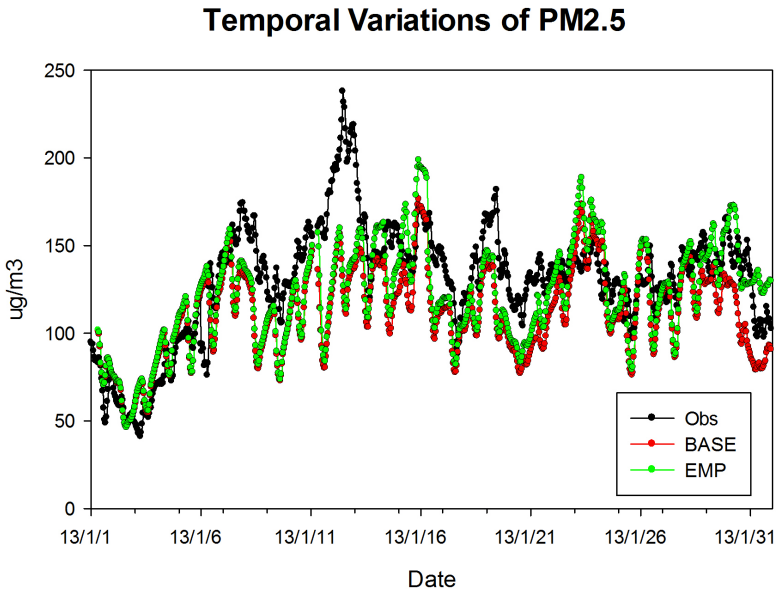

Figure 6. Comparison of observed (black) and simulated (red for scenario BASE and blue for scenario EMP) hourly near surface $PM_{2.5}$ mass concentrations averaged over 71 cities in China in January 2013.

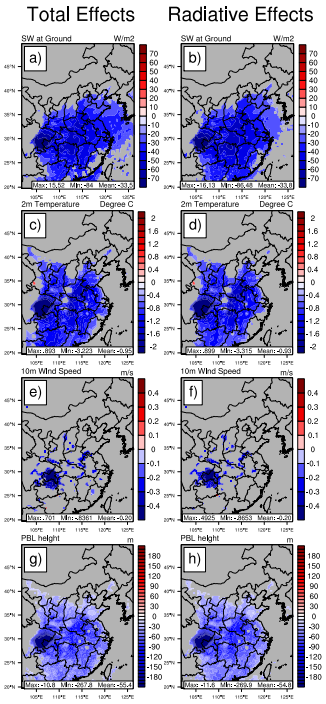

Figure 7. Simulated aerosol total effects (scenario BASE – EMP) and radiative effects (scenario RAD – EMP) on downward short wave flux at ground, 2 m temperature, 10 m wind speed and PBL height in January 2013.The aerosol indirect effects on these four meteorological variables are not shown here, since the induced changes are not significant according to Student's *t* test. Grey shaded areas indicate regions with less than 95 % significance.

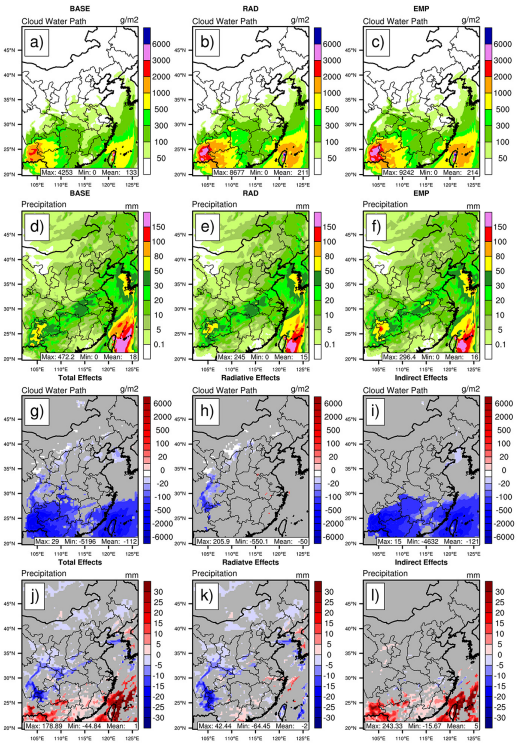

Figure 8. Simulated cloud water path and precipitation for the three scenarios and aerosol total effects (scenario BASE – EMP), radiative effects (scenario RAD – EMP), and indirect effects (scenario BASE – RAD) over eastern China in January 2013. Grey shaded areas indicate regions with less than 95 % significance.

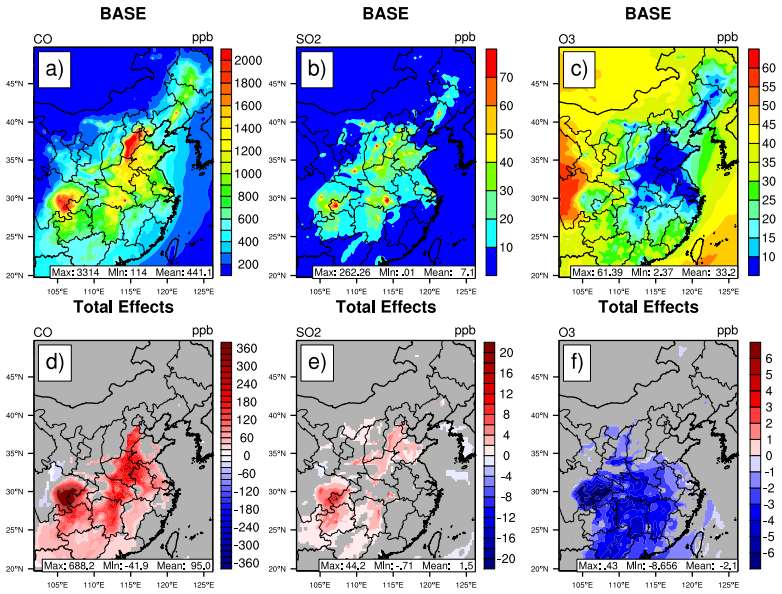

Figure 9. Simulated monthly mean CO, SO_2, and O_3 mixing ratios and aerosol feedbacks (scenario BASE – EMP) on the three gas pollutants over eastern China in January 2013. Grey shaded areas indicate regions with less than 95 % significance.

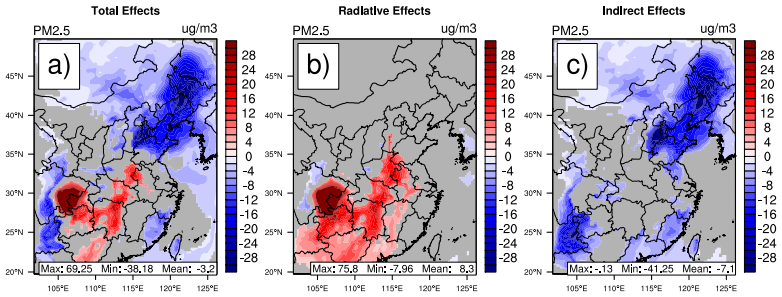

Figure 10. Simulated aerosol total effects (scenario BASE – EMP), radiative effects (scenario RAD – EMP), and indirect effects (scenario BASE – RAD) on monthly mean $PM_{2.5}$ over eastern China in January 2013. Grey shaded areas indicate regions with less than 95 % significance.

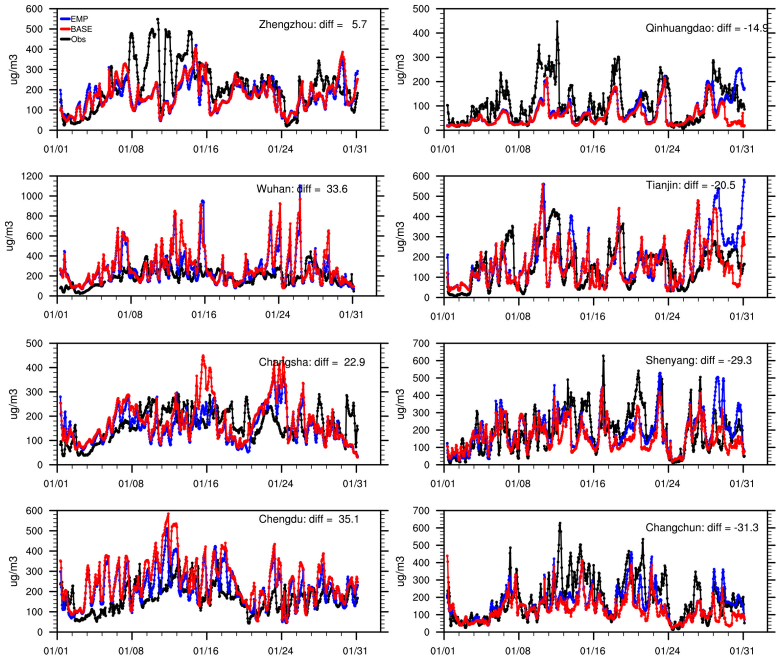

Figure 11. Time series of observed (black) and simulated (red for scenario BASE and blue for scenario EMP) hourly surface $PM_{2.5}$ mass concentrations in 8 cities in January 2013. Monthly mean $PM_{2.5}$ are enhanced in the four cities (Zhengzhou, Wuhan, Changsha and Chengdu) in the left column. Cites in the right column have suppressed monthly mean $PM_{2.5}$ mass concentrations. "Diff" indicates aerosol feedbacks (BASE – EMP) on monthly mean $PM_{2.5}$ mass concentrations.

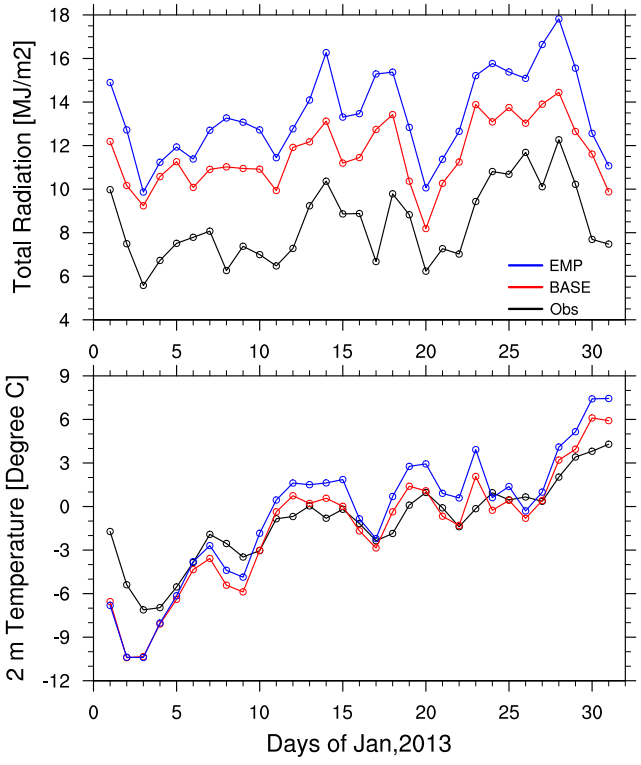

Figure 12. Time series of observed (black) and simulated (red for scenario BASE and blue for scenario EMP) daily total radiation and 2 m temperature averaged over North and central China in January 2013.

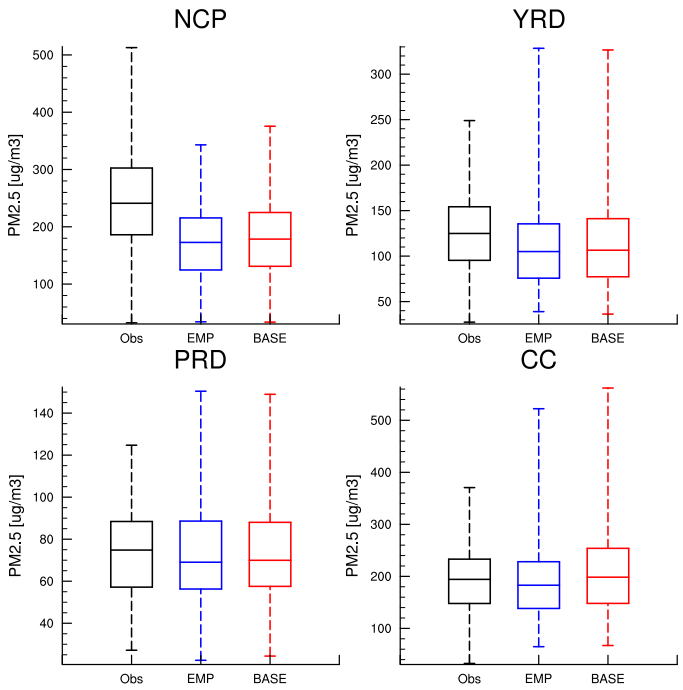

Figure 13. Observed (black) and Simulated (red for scenario BASE and blue for scenario EMP) monthly mean $PM_{2.5}$ mass concentrations in January 2013 over the North China Plain (NCP), the Yangtze River Delta (YRD), the Pearl River Delta (PRD) and Central China (CC). The dashed lines indicate the maximum and minimum value. The solid lines in the box indicate the median value (the central line), the 25th and 75th percentiles.